fishes

MDPI

Article

Mass Selection and Computer Vision-Based Phenotyping of Shell and Mantle Edge Color in Brazilian Black-, Golden-, and White-Shelled Pacific Oyster Strains

Carlos Manoel do Espírito Santo [1,*], Carlos Henrique Araujo de Miranda Gomes [1], Alexandra Inês dos Santos [1,2], Vinícius Mikio Suzuki [1] and Claudio Manoel Rodrigues de Melo [1]

[1] Laboratory of Marine Mollusks, Department of Aquaculture, Federal University of Santa Catarina, Rua dos Coroas, 503, Florianópolis 88061-600, SC, Brazil; carloshenriquelabmol@gmail.com (C.H.A.d.M.G.); alexandrasantos@epagri.sc.gov.br (A.I.d.S.); vinicius.m.suzuki@gmail.com (V.M.S.); claudio.melo@ufsc.br (C.M.R.d.M.)

[2] Company of Agricultural Research and Rural Extension of Santa Catarina, Itajaí 88318-112, SC, Brazil

* Correspondence: carlos.mes@ufsc.br

Abstract

Shell color in *Crassostrea gigas* (syn. *Magallana gigas*) is a trait of both genetic and commercial importance. In this study, we derived black-, golden-, and white-shelled strains through mass selection over five generations from a genetically restricted, geographically isolated South American (Brazilian) base population. To assess selection effectiveness and the relationship between shell and mantle edge color, we compared these strains with a control group derived from the founder population. Shell and mantle edge colors were quantified using CIELAB L^*, a^*, b^*, and ΔE parameters. All selected strains differed significantly from the control and from each other ($p < 0.05$), except for mantle edge b^*, which did not differ between the white strain and the control. The golden strain exhibited the lowest phenotypic uniformity, with a significantly higher ΔE than the black and white strains. Positive and significant Pearson correlations for L^* between shell and mantle edge color were observed within strains (mean r = 0.43) and across the control (r = 0.67). Principal component analysis of color parameters revealed distinct clustering. Black and white strains were more uniform, while the control showed greater phenotypic diversity. Mass selection effectively developed distinct shell-color phenotypes and resulted in a correlated phenotypic response in mantle edge coloration.

Keywords: shell pigmentation; bivalve; *Crassostrea gigas*; *Magallana gigas*; CIELAB; genetic improvement

Key Contribution: This study provides evaluation of mass selection for shell color applied simultaneously to establish black, golden, and white shell strains from a geographically isolated South American (Brazilian) base population of *Crassostrea gigas*. Using a CIELAB computer vision model, it demonstrates that mass selection effectively standardizes shell color phenotypes while driving a correlated response in mantle edge pigmentation. It also reveals distinct standardization efficiencies among color morphs, with black and white strains achieving higher uniformity than the golden strain.

Check for updates

Academic Editors: Yuanzi Huo and Emily Kunselman

Received: 25 September 2026
Revised: 9 November 2026
Accepted: 10 November 2026
Published: 17 November 2026

Copyright: © 2026 by the authors. Licensee MDPI, Basel, Switzerland. This article is an open access article distributed under the terms and conditions of the Creative Commons Attribution (CC BY) license.

1. Introduction

Shell color in the Pacific oyster, *Crassostrea gigas* (Thunberg, 1793) (syn. *Magallana gigas*), is a phenotypic trait of significant genetic and commercial relevance. The shell of

this species exhibits broad pigmentation polymorphism, ranging from completely white to entirely black [1]. Imai and Sakai [1] pioneered the study of this trait's heritability, observing that the offspring of black-shelled oysters were more likely to inherit this color. Subsequently, studies aiming to diversify products in the U.S. West Coast oyster market demonstrated that shell and mantle edge color are primarily determined by genetic effects [2]. Since then, other studies have reported high narrow-sense heritability (h^2) for shell color (up to 77%) [3,4] and similarly high broad-sense heritability (H^2) for mantle edge color [4,5]. Furthermore, significant positive genetic correlations of up to 0.92 have been observed between these phenotypic traits [2,4,5].

Although some studies suggest no consistent correlation between shell color and growth and survival [6], the genetic correlation between these traits is inconsistent across different strains [7]. Nevertheless, biological explanations for performance differences in oysters with varying shell colors have been identified. For instance, black shell pigmentation may confer greater immune competence and enhanced oxidative stress response strategies compared to white shell pigmentation [8]. Furthermore, a study on the related oyster species *C. angulata* showed that triploids of the black-shelled lineage had greater tolerance to elevated temperatures, outperforming the golden and normal lineages [9].

The potential of shell color as a commercial trait has driven genetic studies, particularly in *C. gigas* [7]. However, the phenotypic diversity of shells has been most extensively explored in China, to which the species is native. Family selection has enabled the development of strains with white, black, gold, purple [10], and orange [11] shells from wild and cultivated individuals. Although various authors have reported progress in establishing these strains, the process is costly, as it requires managing a large number of families over several generations [5,11–16].

Conversely, mass selection is particularly suitable for improving a single trait, particularly one with high heritability [17]. This selection method is considerably simpler and less costly than methods based on individual tagging and pedigree records [18]. Furthermore, an essential requirement for either mass or individual selection is the ability to measure the trait in the living broodstock [19]. Based on these premises, shell color is an ideal trait for individual selection.

Shell color is typically the result of biological pigments that reflect or transmit specific wavelengths of light [20]. Initially, studies on this trait in *C. gigas* relied on visual categorization, grouping shells by different pigmentation levels, ranging from completely light to dark [1,2,4]. However, a significant breakthrough occurred when Evans et al. [3] introduced digital analysis using a computer vision system, a methodology that has since been adopted in subsequent studies.

Among the digital methods for food color assessment, the *L**, *a**, and *b** color model is the most suitable for curved surfaces [21], such as those of Pacific oyster shells. This system, known as the CIELAB color model, was adopted as the international standard for color measurement by the *Commission Internationale d'Eclairage* (CIE) in 1976 [22]. CIELAB provides a color representation consistent with human perception, regardless of the devices used for image capture and display, making it ideal for food science research [22]. For these reasons, it has been adopted to assess shell color in *C. gigas* strains, with conclusive results reported by Wan et al. [13] and Xu et al. [16].

Although selective breeding for dark shell color has been previously conducted in Asian *C. gigas* populations using family selection followed by mass selection for growth [15], this study applied mass selection to shell color since the first generation to simultaneously establish black, golden, and white strains from a historically isolated South American (Brazilian) base population. It also provides a quantitative assessment that integrates

CIELAB color parameters (L^*, a^*, b^*, ΔE) across shell and mantle edge tissues in selected strains relative to an unselected founder control group.

2. Materials and Methods

2.1. Mass Selection and Experimental Design for Strain Comparison

The selection of three groups of *C. gigas* with black, gold, and white shells began in October 2019, using the mass selection method. Thereafter, each group was bred in isolation under individual selection programs and was subsequently designated as a strain. The sole selection criterion for all three strains over five generations was the color of the left and right shell valves [23]. Concurrently, an unselected control group was maintained through random mating across all five generations under the same cultivation conditions as the strains (see Table S1 for details). The broodstock and genetic base for developing these strains were sourced from the Laboratory of Marine Mollusks at the Federal University of Santa Catarina, which holds the sole pedigree-controlled *C. gigas* broodstock in Brazil [24,25].

To reproduce each generation in the laboratory, a gamete pool was created using 25 males and 25 females from each strain. Spawning was induced by stripping the gametes, following the method described by Helm and Millican [26]. External fertilization, egg incubation, and larviculture in a static and recirculation system were conducted according to the protocols described by Helm et al. [27] and Ramos et al. [28], respectively. During the final larval stage, from the pediveliger phase onward, the method described by Gomes et al. [29] was used until the spat were retained on a 1.5 mm mesh for transfer to the sea. For the experimental design, each strain and the control group came from a distinct mass spawning batch. They were reared in a single larviculture and a single settlement tank, with no replication during the hatchery phase (Table S1).

Over five generations, the spat were cultured at sea on a long-line system in Sambaqui, North Bay, Florianópolis, Santa Catarina, Brazil (27°29′18″ S; 48°32′12″ W). 10,000 spat, retained on a 1.5 mm mesh, from each strain and control group were cultured in two floating wood culture boxes with a 1.5 mm mesh size (between knots) as described by Lima et al. [30]. After approximately 35 days of culture, 2800 golden and 1960 black and white strains and control group of oyster spat randomly collected were transferred to lantern nets. Each lantern net consisted of four tiers, with each tier measuring 0.13 m^2. The grow-out process followed the methodology described by Sühnel et al. [31], encompassing the nursery, intermediate, and final phases, using lantern nets as replicates of the cultivation units randomly distributed along the floating long-line suspended at the surface (Table 1).

Table 1. Initial stocking densities and allocation of the culture units (lantern nets) across the nursery, intermediate, and final grow-out phases at sea for the selected strains and the control group of *Crassostrea gigas*.

Genetic group	Number of Oysters	Cultivation Phase	Mesh Size (mm)	Oysters Tier^{-1}	Oysters Lantern^{-1}	Number of Replicates
Black, White, and Control	1960	Nursery	4	245	980	2
		Intermediate	18	98	392	5
		Final	30	61	245	8
Golden	2800	Nursery	4	233	933	3
		Intermediate	18	100	400	7
		Final	30	64	255	11

Selection of broodstock for the next generation began when oysters transitioned from the intermediate to the final grow-out phase, reaching 5.0 cm in length. The selection

involved choosing 50 individuals with the desired phenotype from a population of 1960 for the black and white strains, and from a population of 2800 for the golden strain. This corresponded to a selected proportion (p) of 2.6% for the black and white strains and 1.8% for the golden strain, and selection intensity (i) $i = \frac{Z}{p}$ of 2.33, and 2.46, respectively.

Given the balanced sex ratio of the pooled breeders (25 males and 25 females), the theoretical effective population size (N_e) was maintained at 50 per generation for each strain.

The experiment involved phenotyping the fifth generation (G5) of each strain using a computer vision system and the *L*a*b** color space. The treatment groups consisted of the black, golden, and white shell strains (Figure 1). The control group, an unselected base population representing the initial stock, served as the phenotypic reference for the selected strains (Figure 2).

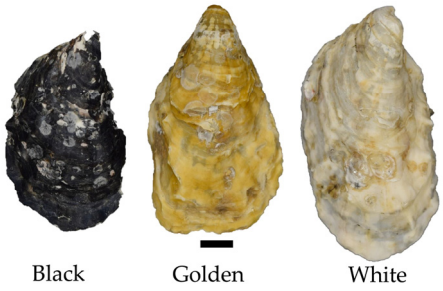


Figure 1. Left valve of color reference specimen for *Crassostrea gigas* shell strains (scale = 1 cm). Black (L^* = 18.91, a^* = 1.51, and b^* = 0.4); Golden (L^* = 60.76, a^* = 5.31, and b^* = 38.17); White (L^* = 67.94, a^* = 2.0, and b^* = 17.58).

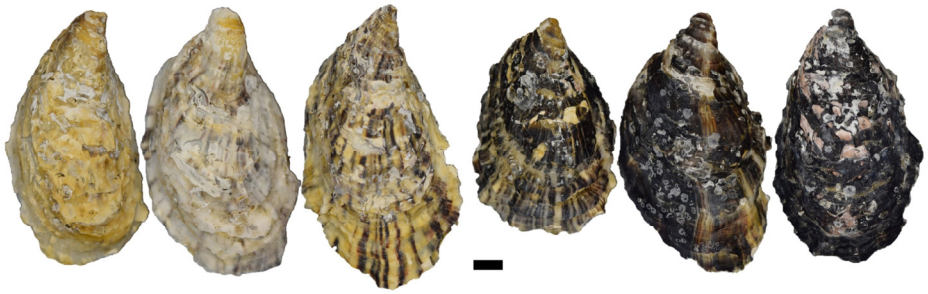


Figure 2. Phenotypic diversity of the left valve of the control group *Crassostrea gigas* oysters, descendants of the founding population of strains (scale = 1 cm).

In June 2024, after 154 days of culture, 100 individuals from the G5 generation of each strain and the control group were randomly sampled in all lantern net replicates for image acquisition and shell color analysis (totaling 400 oysters). After processing, individuals with excessive encrustation and physical damage to the shell or mantle edge, which prevented the precise extraction of the region of interest (ROI), were excluded. The final dataset analyzed comprised 378 individuals: control (n = 100), black (n = 82), gold (n = 96), and white (n = 100).

2.2. Image-Based Phenotyping

The imaging setup and the choice of the CIELAB color space for curved food surfaces were adapted from Mendoza et al. [21] and Yam & Papadakis [22] and followed the protocols established by Wan et al. [13], Xing et al. [5], and Zhang et al. [32] for color measurement in *C. gigas* oyster shells, as described below. Images were captured using a Nikon D3300 camera (Nikon Corporation, Tokyo, Japan) with a 24.2-megapixel sensor, using the following

settings: F/5.6 aperture, 46 mm focal length, 1/160 s shutter speed, and ISO 200. Exposure was set to 0 (EXP 0), with the flash disabled and focus set manually. White balance was manually calibrated prior to image acquisition using a standard neutral white reference card.

The camera was mounted on a tripod and positioned approximately 28 cm above the sample inside a photo light box with a matte black background. The light box was illuminated by four 9 W LED bulbs with a color temperature of 6500 K. The bulbs were positioned 20 cm above the sample at the four corners of a 45 cm square, creating an approximate 45° angle of incidence between the light axis and the sample. For image acquisition, the camera was connected to a computer via USB and operated remotely using digiCamControl (v2.1.6.0). The images were taken at 4000 × 6000 pixels, and 300 dpi, and saved in JPG format.

The shells and mantle edges were photographed immediately after harvest. Prior to photography, the shells were lightly brushed with a 5% sodium hypochlorite solution and rinsed with freshwater to remove superficial mud, microalgal biofilms, and loose biofouling without altering the underlying mineralized shell pigmentation, following established bivalve phenotyping protocols [3,16,23].

The images were analyzed using Adobe Photoshop 2022 (Adobe Inc., San Jose, CA, USA) to obtain Lightness, a, and b values from the histogram window based on the sRGB color profile, which natively operates under the CIE Standard Illuminant D65 and the CIE 1931 2° Standard Observer. These digital values (ranging from 0 to 255) were then converted to the standard CIELAB coordinates L^*, a^*, and b^* as described by Yam and Papadakis [22], using the following equations:

$$L^* = \frac{Lightness}{255} \times 100$$

$$a^* = \frac{240a}{255} - 120$$

$$b^* = \frac{240b}{255} - 120$$

For the shell color analysis, the region of interest (ROI) was defined as the entire surface of the left valve, excluding any areas with biofouling, as described by Xu et al. [16]. The ROI for the mantle edge was selected based on the criteria of Li et al. [33], as shown in Figure 3.

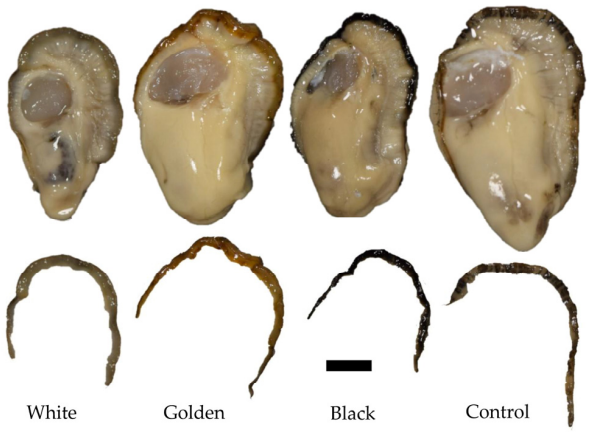


Figure 3. Mantle and respective regions of interest (ROI) of the mantle edge for black golden, and white strains, and control group, used to obtain the color parameters L^*, a^*, and b^* (scale = 1 cm).

In the CIELAB color model, L^* represents lightness (0 = black, 100 = white), while a^* ranges from −120 (green) to +120 (red), and b^* ranges from −120 (blue) to +120 (yellow) [22]. These parameters were determined for the shell and mantle edge of every

individual in the sample. The total color difference (ΔE) of the shells was calculated from these components using the equation described by Chakraborty et al. [34]:

$$\Delta E = \sqrt{\left(L^* - L_i^*\right)^2 + \left(a^* - a_i^*\right)^2 + \left(b^* - b_i^*\right)^2}$$

ΔE measures the distance between two colors within the CIELAB model. The ΔE for each strain (ΔE_B for black, ΔE_G for golden, and ΔE_W for white) is calculated as the average difference between each individual and the strain's standard specimen (Figure 1). The reference specimens for the black, golden, and white strains (Figure 1) were selected from the G5 generation considering a solid target morphotype for each strain, free from stripes, secondary colorations, or shell deformities. Where L^*, a^*, and b^* are the color parameter values for each individual's shell, and L_i^*, a_i^*, and b_i^* are the values for the standard specimen of each strain. Therefore, a lower ΔE value indicates a more homogeneous strain with respect to the desired phenotype.

For the control group, a single representative specimen could not be defined due to the high variability in shell color (Figure 2). Consequently, three ΔE parameters were calculated: ΔE_{CB}, ΔE_{CG}, and ΔE_{CW}. These values represent the average color difference between individuals in the control group and the standard specimen of the black, golden, and white strains, respectively. Therefore, a higher ΔE between the control group and each strain's standard individual indicates greater differentiation or distance from the group of oysters not selected for the desired phenotype, and vice versa.

To estimate measurement repeatability, a random subset of 30 shells of individuals across the different genetic groups was blindly re-measured by the same operator, with a mean Coefficient of Variation (CV).

2.3. Statistical Analysis

Data normality and homogeneity of variances were assessed using the Shapiro–Wilk and Levene's tests, respectively. Parametric tests were applied when these assumptions were met. Otherwise, non-parametric tests were adjusted.

To compare the shell color parameters L^*, a^*, and b^* among the strains and the control group an Analysis of Covariance (Rank ANCOVA) was performed, utilizing shell length as a covariate. Following a significant main effect of the genetic group, estimated marginal means on the rank scale were calculated and compared using Tukey's post hoc test.

To compare the mantle edge color parameters L^*, a^*, and b^*, as well as the independent ΔE values among the strains, the non-parametric Kruskal–Wallis test was used, followed by Dunn's test with a Bonferroni correction for multiple comparisons.

The ΔE_B, ΔE_G, and ΔE_W data were analyzed using a Linear Mixed-Effects Model (LMM) with the reference strain as a fixed effect and the individual oyster as a random effect. Pairwise comparisons for the LMM were also conducted using Tukey's post hoc test.

To assess true within-strain phenotypic uniformity, a reference-free multivariate dispersion analysis was conducted for the shell color parameters L^*, a^*, and b^*. The Euclidean distances to the group spatial centroid were calculated and compared among strains using a Permutational Analysis of Multivariate Dispersions (PERMDISP) with 9999 permutations, followed by pairwise comparisons with Bonferroni correction.

The L^*, a^*, and b^* values were subjected to a Pearson correlation analysis to assess the relationship between shell and mantle edge coloration. A pooled within-group correlation was calculated using the residuals of linear models controlling for the strain effect. Additionally, differences in the magnitude of the correlation coefficients among the individual groups were tested using a Chi-square test of heterogeneity based on Fisher's Z-transformations. Pairwise Fisher's Z-tests with Bonferroni correction were subsequently applied to identify specific differences in correlation strength between strains.

Finally, a principal component analysis (PCA) was performed on the combined L^*, a^*, and b^* values of the shell and mantle edge to examine the distribution of individuals from each strain and identify any potential clustering. Prior to the PCA, the data were standardized by subtracting the mean from each value and dividing by the standard deviation.

The Shapiro–Wilk, Levene's, PERMDISP, and PCA analyses were performed using PAST software (version 4.13) (Natural History Museum, University of Oslo, Oslo, Norway) [35]. The LMM was conducted using the lme4, emmeans, and lmerTest packages; Rank ANCOVA was conducted using the car and emmeans packages; a pooled within-group correlation and the chi-square test of heterogeneity based on Fisher's Z-transformations were conducted using the dplyr package, and pairwise Fisher's Z-tests were conducted using the cocor package in R (version 4.4.3) (R Foundation for Statistical Computing, Vienna, Austria). The significance level for all analyses was set at 5% ($p < 0.05$).

3. Results

The repeated manual selection of the ROI in Photoshop yielded a mean Coefficient of Variation (CV) for the L^*, a^*, and b^* parameters of 3.26, 2.24, and 5.09, respectively. Only the ΔE values of the control group (ΔE_{CB}, ΔE_{CG}, and ΔE_{CW}) showed a normal distribution and homogeneous variances, and were therefore analyzed using parametric ANOVA. Non-parametric Kruskal–Wallis test was applied to the L^*, a^*, and b^* values of the shell and mantle edge, as well as to the ΔE_B, ΔE_G, and ΔE_W values.

The Rank ANCOVA revealed that while shell length had a significant covariate effect on the b^* parameter ($p = 0.020$), it did not significantly influence L^* ($p = 0.403$) and a^* ($p = 0.2169$) (see Table S2 for shell height, length, and width). After controlling for shell length, the effect of the genetic strain remained significant across all shell color parameters (Figure 4). The same pattern was observed for the mantle edge, except for the b^* value, where the difference between the control and the white strain was not significant (Figure 4).

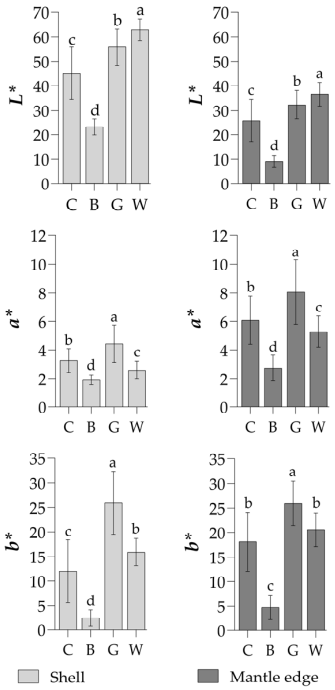


Figure 4. Means ± standard deviation of the color parameters L^*, a^*, and b^* for the shell, and the mantle edge of *Crassostrea gigas* strains: black (B), golden (G), and white (W), and control (C). Different letters above the bars of the shell indicate a significant difference according to Tukey's test, and of the mantle edge indicate a significant difference according to Dunn's test ($p < 0.05$).

The black and white shell strains had significantly lower ΔE values than the golden strain (Figure 5). Within the control group, the ΔE_{CW} value was significantly lower than the ΔE_{CB} and ΔE_{CG} values.

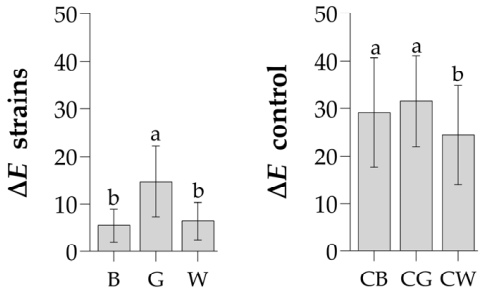


Figure 5. Means ± standard deviation of the chromatic distance (ΔE) for individuals of the *Crassostrea gigas* strains with black (B), golden (G), and white (W) shells relative to their respective standard specimens, and for the control group relative to the standard specimens of the black (CB), golden (CG), and white (CW) strains. Different letters above the bars indicate a significant difference according to Dunn's test for the ΔE of the strains and according to Tukey's test for the ΔE of the control ($p < 0.05$).

The PERMDISP test revealed significant differences in multivariate dispersion for the color shell L^*, a^*, and b^* parameters among the groups (Figure 6). The black and white strains had significantly shorter distances to the centroid than the golden strain, indicating greater phenotypic uniformity in the black and white groups. The golden strain exhibited higher phenotypic variability and did not differ significantly from the unselected control group.

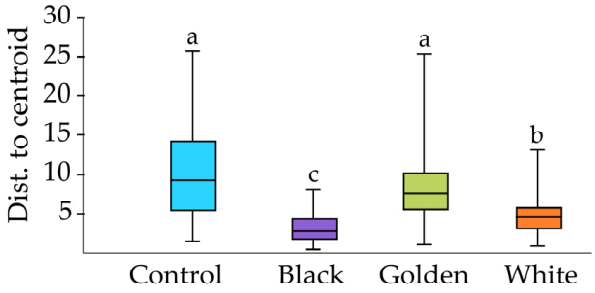


Figure 6. Multivariate dispersion of shell color parameters (L^*, a^*, and b^*) for the selected strains (White, Golden, and Black) and the unselected control group of *Crassostrea gigas*. The boxplots display the Euclidean distances of individual oysters to their respective group spatial centroids, as calculated by the PERMDISP analysis. Different superscript letters on the boxes denote statistically significant differences between groups based on pairwise comparisons with Bonferroni correction ($p < 0.05$).

A significant positive pooled within-group correlation was observed for L^*, a^*, and b^* values between the shell and the mantle edge (Table 2). When analyzing each group separately, the correlation for L^* was positive and significant in all strains and in the control group. For a^* and b^*, the correlation was positive and significant in all groups, except for a^* in the white strain and b^* in the black strain. Furthermore, a formal Chi-square test of heterogeneity based on Fisher's Z-transformations revealed significant differences in the magnitude of the correlation coefficients among the individual groups. Subsequent pairwise comparisons using Fisher's Z-tests with Bonferroni correction demonstrated that the phenotypic correlation was significantly stronger in the control group compared to the strains, primarily for L^* and b^*. However, the correlations among the strains did not show a significant difference.

Table 2. Pearson correlation (r-values) and 95% confidence intervals for r-values between the color parameters *L**, *a**, and *b** of the shell and the mantle edge in *Crassostrea gigas* strains, alongside the Chi-square (X^2) heterogeneity statistic based on Fisher's Z-transformations.

CIELAB Coordinates	Genetic Groups	r-Values	X^2	Confidence Interval (95%)
*L**	All [1]	0.531	15.31	0.455 to 0.600
	Control	0.672 [a]		0.548 to 0.767
	Black	0.298 [b]		0.087 to 0.484
	Golden	0.322 [b]		0.130 to 0.491
	White	0.419 [ab]		0.242 to 0.569
*a**	All	0.248	12.56	0.151 to 0.341
	Control	0.346 [a]		0.160 to 0.508
	Black	0.340 [a]		0.132 to 0.520
	Golden	0.276 [ab]		0.080 to 0.452
	White	−0.083 [b]		−0.275 to 0.115
*b**	All	0.472	18.71	0.390 to 0.547
	Control	0.654 [a]		0.525 to 0.754
	Black	0.176 [b]		−0.043 to 0.379
	Golden	0.333 [b]		0.142 to 0.500
	White	0.317 [b]		0.128 to 0.483

[1] Values in the 'All' row represent the pooled within-group correlation, calculated from the residuals of linear models controlling for the strain effect. Different superscript letters indicate significant differences between independent correlation coefficients for the strains and the control group according to pairwise Fisher's Z-tests with Bonferroni correction ($p < 0.05$).

The dispersion of individuals illustrates these correlations and visually distinguishes the genetic groups (Figure 7).

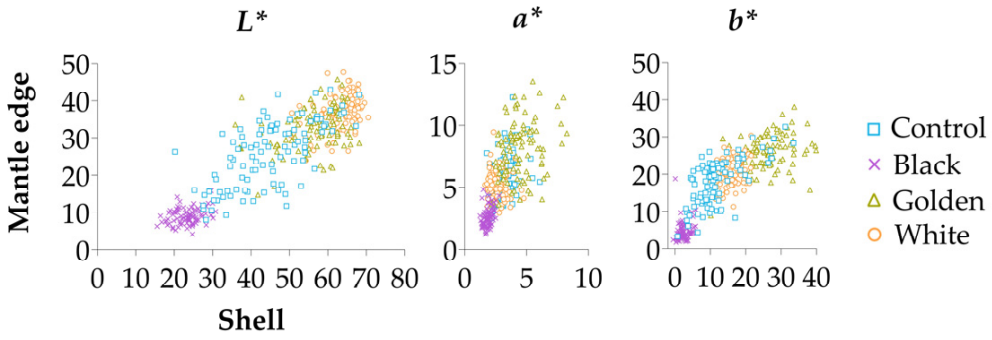


Figure 7. Dispersion of the *L**, *a**, and *b** parameters showing the relationship between the shell color (*x*-axis) and the mantle edge color (*y*-axis) of the *Crassostrea gigas* strains and the control group.

The PCA revealed the distribution of the evaluated individuals, showing the formation of distinct clusters, as well as areas of overlap between the strains and the control group (Figure 8).

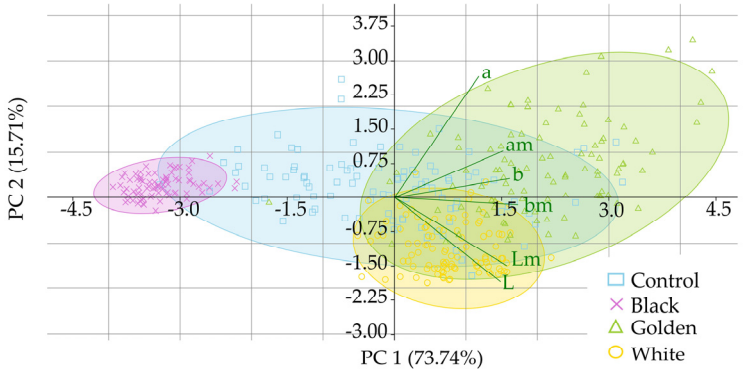


Figure 8. Principal component analysis (PCA) characterizing the black-, golden-, and white-shelled *Crassostrea gigas* strains, and the control group, based on the *L**, *a**, and *b** parameters of the shell color (L, a, and b) and the mantle edge color (Lm, am, and bm). The ellipses represent the 95% data (concentration) ellipses for each group, illustrating the multidimensional phenotypic variance and spatial distribution of the individuals within each strain.

4. Discussion

In Brazil, *C. gigas* is an introduced species, having been repeatedly imported for aquaculture purposes between 1974 and 2008 from Great Britain, Japan, France, the United States, and Chile [36–38]. Currently, *C. gigas* cultivation in Brazil relies exclusively on hatchery-produced seeds derived from a single broodstock, since there is no collection of wild seeds [25,31]. The genetic diversity of this founder population, which served as the base for the strains selected in this study, was previously assessed using microsatellite markers, revealing an average of 7 alleles per locus and an expected heterozygosity (He) of 0.62 [39]. Although historical isolation has reduced the genetic diversity indices of this broodstock compared to other worldwide cultivated populations, the maintained batch still preserves levels of variability comparable to those of other base populations utilized in the selection of strains with distinct shell colors [13,15,39]. Furthermore, the present study demonstrated the maintenance of phenotypic diversity regarding individual coloration within this broodstock, providing evidence that mass selection was effective in segregating of groups with black, golden, and white shells and mantle edges.

The standardized setup, combined with sRGB-to-CIELAB transformation equations, allowed for reliable comparisons among strains and the control group, as demonstrated in previous studies [5,13]. The CIELAB coordinate values obtained in this study represent relative chromatic variations within the sample batches, rather than absolute reflectance values. Comparisons with the results of other studies are not definitive and were made with some caution. High repeatability, confirmed by repeated manual selection of the ROI in Photoshop, indicates minimal operator-introduced variance during image extraction.

The highest mean values of *L** were found in the golden and white strains. The black shell strain, which is more pigmented, had the lowest values. The control group exhibited the second-lowest mean *L** value, likely due to a higher prevalence of shells with dark stripes in this group. All groups had shells with *a** values very close to the achromatic region, minimizing the importance of this component in distinguishing between the strains. However, the *b** component, associated with yellow in human vision, was relevant for distinguishing the golden strain from the other groups.

The mean *L**, *a**, and *b** values of the golden-shelled oysters were similar to the results of Zhang et al. [32], who also evaluated the twelfth generation and obtained values of 54.26, 6.24, and 36.67, respectively. However, we recorded a ΔE_G value 1.9 times higher than that reported by these authors, likely reflecting the different selection methods used and the number of generations of selection. Furthermore, family selection, used for four generations,

allowed for the culling of families with undesirable phenotypes [32], an advantage not offered by individual selection.

Crossing golden-shelled oysters produces offspring with a Mendelian segregation ratio of approximately 3:1 [12]. This trait is controlled by a single locus with two alleles, where the dominant allele is responsible for the golden color and the recessive allele for the white color [12]. In the present study, we identified individuals with off-white shells among the offspring of the golden strain. However, no individuals sampled from the offspring of the white strain exhibited the golden phenotype, which corroborates the findings of Ge et al. [12]. Other studies also did not observe the golden phenotype in crosses between white-shelled oysters, reporting that the white shell phenotype tends to produce predominantly white offspring or those with some degree of dark pigmentation [3,14].

Furthermore, the higher ΔE_G value observed between the strains in the present study may be attributed to the greater prevalence of dark-pigmented stripes in the golden strain than in the white-shelled strain. This, in turn, may be an epistatic effect between the genes that control golden and dark pigmentation [12]. However, information regarding the segregation and genetic inheritance of the golden and black shell phenotypes is still lacking in the literature. The more complex inheritance pattern of the golden phenotype, as suggested by Ge et al. [12], still requires further investigation.

Our results of CIELAB coordinates, and ΔE_W for white-shelled are consistent with those of Zhang et al. [32]. Furthermore, we have shown that individuals from the white and black-shelled strains are closer to their respective standard phenotypes than the golden strain. This indicates greater phenotypic uniformity in these strains. The golden-shelled strain, on the other hand, was more challenging to develop, resulting in animals that were less homogeneous for this trait. These results were observed in the first-generation offspring, when we applied a higher selection intensity to the golden-shelled strain.

Multivariate dispersion analysis of L^*, a^*, and b^* values mathematically confirmed that mass selection increased the phenotypic uniformity of the black and white strains compared to the control, whereas the golden strain maintained high variability.

The high phenotypic variability observed in the control group, which is descended from the strains' founder population, includes individuals with light (white and golden), dark, and striped shells. This suggests that this group may be phenotypically similar to the wild and cultivated populations from which the strains were originally selected in China [10]. Among all strains studied, the white-shelled strain exhibited the lowest ΔE_{CW} and, consequently, the greatest proximity to the control group in the CIELAB color model. The a^* and b^* values for the shells appear to have been the decisive factors in the lower ΔE_{CW}. The b^* value contributed to the higher ΔE_{CG}, increasing the golden strain's distance from the control. In the black-shelled strain, the lower L^* value determined the increase in its ΔE_B relative to the control group.

To our knowledge, this is the first study to evaluate the relationship between shell and mantle edge color in *C. gigas* using the L^*, a^*, and b^* coordinates of the CIELAB color model. It is also the first study to investigate this correlation in a golden-shelled strain. Although Nell [40] observed that golden-shelled *C. gigas* individuals tend to have an orange/bronze mantle edge, the present study aimed to expand on this analysis using a quantitative approach.

For comparison with findings from other studies, we considered the correlation between the L^* values of the shell and the mantle edge to be the most suitable metric. Since L^* is strongly correlated with the optical density (OD) of oyster shells [16], one study detected a significant positive correlation ($r = 0.423$) between shell OD and spectrophotometric pigment readings in white-shelled families [5]. Furthermore, a significant positive correlation

($r = 0.578$) was identified when assessing pigmentation level categories across black- and white-shelled *C. gigas* families [2].

To avoid artificial inflation driven by differences among strain means, a pooled within-group correlation was calculated, indicating that the strength of the association between shell and mantle color is strain-dependent. The significant positive correlation between shell and mantle edge color in the control group indicates a strong relationship between these two phenotypic traits. However, this relationship was altered by the selection process, as the strength of the correlation varied considerably among the genetic groups studied. These findings suggest that the greater the phenotypic variability, the stronger the observed correlation.

In the control group, phenotypic variation for shell and mantle edge color is high, resulting in a strong correlation between these traits. As selection pressure is applied for a specific trait, the phenotypic variability for that trait is reduced. This reduction in variance introduces a statistical restriction of range within the selected groups. Since shell and mantle edge color are related in *C. gigas* [33], reducing the variability in shell color also reduces the variability in the mantle edge, which lowers the covariance between them and results in smaller Pearson correlation coefficients (r).

Furthermore, the lower r in the selected strains suggest that there is potential to strengthen this correlation if selecting for a uniform mantle edge color is an objective. However, it would be valuable to test the effect of reverse selection based on mantle edge color. Given that numerous studies have already conducted selection experiments based on shell color, the relationship between these traits appears to be well-established [2,4,5,33].

Regarding the shell color standardization, the multivariate dispersion analysis provided reference-free evidence of phenotypic uniformity. The significantly lower centroid distances in the black and white strains demonstrate that mass selection successfully constrained shell color variation. In contrast, the golden strain exhibited higher dispersion, indicating a persistent phenotypic variability comparable to the unselected control.

The PCA results indicated a correlation between the shell and mantle edge color variables, as shown by the angle between their vectors. The strongest correlation was observed for L^*, followed by b^* and a^*. The PCA results are robust, with the first two principal components explaining 89.45% of the total variance (PC1 73.74% and PC2 15.71%). Similarly, the two main components explained 87.7% of the variation in shell color [32]. When evaluating the global multivariate phenotype (combining both shell and mantle edge color parameters), the Principal Component Analysis (PCA) illustrated a clear spatial divergence among the selected groups. The black and white strains formed distinct, concentrated clusters, suggesting a concurrent phenotypic response in both shell and mantle traits. The broader 95% concentration ellipse of the golden strain further reflects its bigger phenotypic distribution.

The control group was the only one to overlap with all strains, its distribution spanning the positive and negative values of both principal components. The center of the control group's ellipse was approximately at the origin of the two components, which is consistent with its descent from the founder population for the other strains. The ellipse for the white-shelled individuals showed the greatest overlap with that of the control group, indicating a higher degree of phenotypic similarity between these two genetic groups. This result underscores the importance of using the ΔE value to determine the degree of differentiation between the control group and the strains.

As expected, individuals from the black-shelled strain showed a negative correlation with the L^* variable, as lower L^* values indicate darker pigmentation. While seemingly obvious, it is important to note that the PCA distributed individuals along the principal components based on the data for each variable. For example, while the black-shelled strain was negatively correlated with b^*, this does not imply the presence of a bluish phenotype,

as its b^* values remained near zero and thus achromatic on a scale ranging from −120 to +120. This finding, therefore, highlights the importance of interpreting PCA results in conjunction with other analyses. In contrast, individuals from the white-shelled strain showed the highest positive correlation with L^* among all the groups. The golden-shelled strain had the second-highest mean L^* values; however, because PCA considers all color parameters simultaneously, the yellow hue (represented by b^*) was crucial for the cohesion and distinction of this group.

Analysis of the PCA ellipse areas showed that the white- and black-shelled strains form more phenotypically homogeneous groups. A dominance effect for the pigmented phenotype (black over white) has been previously reported, with a predominance of striped over white shells, which is consistent with our finding that the white strain's ellipse is larger than the black's [3,14]. Despite the greater selection intensity applied, the golden-shelled strain showed higher phenotypic variability compared to the other strains. This is reflected in the strain's larger ellipse, its higher recorded ΔE_G value, and a higher centroid distance in multivariate dispersion. Furthermore, there was an overlap between the ellipses of the golden and white lineages. Our b^* values in the white lineage and ΔE_G values in the golden lineage, which were comparatively higher than those of Zhang et al. [32], may explain this overlap, which was absent in the study by those authors.

Each strain was produced from separate spawning batches and reared in a single larval-rearing tank, with no replication at the production-unit level, due to the limitations inherent in managing multiple mass-selected strains. Consequently, the genetic strain effect is inherently confounded with minor environmental variations specific to the larval tanks or spawning timing. However, it is established in the literature that shell color in *C. gigas* is a highly heritable trait predominantly driven by strong genetic control [3,4,11,16,23]. While the theoretical effective population size (*Ne*) was maintained at 50 per generation for all strains, the highly variable reproductive success typical of bivalves means the realized *Ne* may be lower. Future genomic analyses will be necessary to estimate the true rate of inbreeding and genomic diversity within these strains.

Despite the successful development of these phenotypically distinct groups of black, golden, and white shells and the advantages of individual selection over family selection (primarily concerning production and labor costs), the disadvantages must also be considered. The high fecundity of bivalves, combined with the possibility that only a few individuals will contribute offspring to subsequent generations [41], leads to a loss of genetic variability, which can negatively affect the oysters' performance and production traits. This loss of variability can also lead to increased inbreeding [42]. Although the theoretical effective population size (*Ne*) per generation is small, the maintenance of phenotypic variability and heterozygosity reported by Scaranto et al. [39] supports the maintenance of lineages in the short term. Furthermore, these detrimental effects can be more easily mitigated in oysters by adopting family selection [19] or a combination of the two breeding strategies [17]. Future work should address these issues and also include additional phenotypic traits, particularly growth and survival.

In summary, the results of this study demonstrate a correlation between shell and mantle edge color parameters within the CIELAB model. Our results corroborate previous findings and suggest that mass selection based on shell color is a viable strategy for altering mantle edge color, and vice versa. Furthermore, our findings expand the current understanding of the golden-shelled strain, reinforcing the importance of the b^* component in its phenotypic differentiation. The PCA confirmed the distinction between the strains across the entire CIELAB color model and highlighted the greater phenotypic variability of the golden strain, suggesting a more complex inheritance pattern for this color than for the white- and black-shelled strains.

5. Conclusions

The computer vision system methodology, based on the CIELAB color model, was effective in characterizing and differentiating the black, golden, and white strains from the original population. Mass selection successfully produced phenotypically distinct groups for shell and mantle edge color in *C. gigas*. Individual selection for shell color also altered the mantle edge color. The purification of these lines restricted intra-strain phenotypic variance, depressing the direct shell–mantle color correlations within selected groups compared to the control. The results demonstrate a strong phenotypic association between shell and mantle edge traits, but achieving highly uniform coloration across both structures in breeding lines may require direct selection targeting mantle traits. The white- and black-shelled strains exhibited greater phenotypic homogeneity than the golden-shelled strain, which showed less phenotypic standardization toward color standardization.

Supplementary Materials: The following supporting information can be downloaded at: https://www.mdpi.com/article/10.3390/fishes11110672/s1, Table S1: Summary of the breeding history, larviculture parameters, and selection metrics for the control group and solid-color strains (Black, Golden, and White) of *Crassostrea gigas* over five generations (G1–G5); Table S2: Mean and standard deviation of the shell height, length, and width for the unselected control group and the selected color shell strains of *Crassostrea gigas*.

Author Contributions: C.M.d.E.S.: Writing—review and editing, Writing—original draft, Project administration, Methodology, Investigation, Formal analysis, Data curation, Conceptualization. C.H.A.d.M.G.: Writing—review and editing, Project administration, Methodology, Investigation, Conceptualization. A.I.d.S.: Writing—review and editing, Writing—original draft, Methodology, Investigation, Conceptualization. V.M.S.: Writing—review and editing, Methodology, Investigation, Data curation. C.M.R.d.M.: Writing—review and editing, Writing—original draft, Funding acquisition, Supervision, Investigation, Conceptualization. All authors have read and agreed to the published version of the manuscript.

Funding: This research was funded by the Coordenação de Aperfeiçoamento de Pessoal de Nível Superior—Brazil (CAPES)—Finance Code 001, the Universidade Federal de Santa Catarina (249/2016), and by Conselho Nacional de Desenvolvimento Científico e Tecnológico—Brazil (CNPq) (305807/2022-6).

Institutional Review Board Statement: The study involved bivalves; studies involving invertebrate animals do not need ethical approval.

Data Availability Statement: The original data presented in the study are openly available in Mendeley Data at DOI: 10.17632/v69gv4t5zc. and URL: https://data.mendeley.com/datasets/v69gv4t5zc/1, accessed on 2 September 2026.

Acknowledgments: The authors thank Francisco Carlos da Silva for his methodological instructions and support in spawning and larviculture, to João Paulo Ramos Ferreira for his collaboration in the discussion of the results and PCA, to Lucas Matheus Macedo dos Santos for his assistance in larviculture and preparation of samples for photography, to Alaine Carneiro da Silva for his support in larviculture, and to Josué de Oliveira for his care of the strains at the marine farm. Also, the authors thank the Brazilian National Council for Scientific and Technological Development for the Productivity scholarship awarded to Claudio Manoel Rodrigues de Melo.

Conflicts of Interest: The authors declare no conflicts of interest. The funders had no role in the design of the study; in the collection, analyses, or interpretation of data; in the writing of the manuscript; or in the decision to publish the results.

Abbreviations

The following abbreviations are used in this manuscript:

CIELAB	International Commission on Illumination *L*a*b**
RGB	red, green, blue
ROI	region of interest
PCA	principal component analysis
OD	optical density

References

1. Imai, T.; Sakai, S. Study of Breeding of Japanese Oyster, *Crassostrea gigas*. *Tohoku J. Agric. Res.* **1961**, *12*, 125–171.
2. Brake, J.; Evans, F.; Langdon, C. Evidence for Genetic Control of Pigmentation of Shell and Mantle Edge in Selected Families of Pacific Oysters, *Crassostrea gigas*. *Aquaculture* **2004**, *229*, 89–98. [CrossRef]
3. Evans, S.; Camara, M.D.; Langdon, C.J. Heritability of Shell Pigmentation in the Pacific Oyster, *Crassostrea gigas*. *Aquaculture* **2009**, *286*, 211–216. [CrossRef]
4. Kang, J.-H.; Kang, H.-S.; Lee, J.-M.; An, C.-M.; Kim, S.-Y.; Lee, Y.-M.; Kim, J.-J. Characterizations of Shell and Mantle Edge Pigmentation of a Pacific Oyster, *Crassostrea gigas*, in Korean Peninsula. *Asian-Australas. J. Anim. Sci.* **2013**, *26*, 1659–1664. [CrossRef]
5. Xing, D.; Li, Q.; Kong, L.; Yu, H. Heritability Estimate for Mantle Edge Pigmentation and Correlation with Shell Pigmentation in the White-Shell Strain of Pacific Oyster, *Crassostrea gigas*. *Aquaculture* **2018**, *482*, 73–77. [CrossRef]
6. Han, Z.; Li, Q.; Liu, S.; Kong, L. Crossbreeding of Three Different Shell Color Lines in the Pacific Oyster Reveals High Heterosis for Survival but Low Heterosis for Growth. *Aquaculture* **2020**, *529*, 735621. [CrossRef]
7. Mizuta, D.D.; Wikfors, G.H. Seeking the Perfect Oyster Shell: A Brief Review of Current Knowledge. *Rev. Aquac.* **2019**, *11*, 586–602. [CrossRef]
8. Wei, L.; Jiang, Q.; Cai, Z.; Yu, W.; He, C.; Guo, W.; Wang, X. Immune-Related Molecular and Physiological Differences between Black-Shelled and White-Shelled Pacific Oysters *Crassostrea gigas*. *Fish. Shellfish Immunol.* **2019**, *92*, 64–71. [CrossRef]
9. Liang, Y.; Hu, H.; Cheng, G.; Xu, C.; Li, Q. Growth, Survival and Thermotolerance of Diploids, Triploids and Tetraploids of the Fujian Oyster *Crassostrea angulata* with Normal, Golden and Black Shell Colors. *Aquaculture* **2024**, *591*, 741131. [CrossRef]
10. Song, J.; Li, Q.; Zhong, X.; Kong, L.; Yu, H. Genetic Diversity and Outlier Loci Detecting of Shell Color Variation in the Pacific Oyster (*Crassostrea gigas*) by SNP Markers. *Aquat. Living Resour.* **2017**, *30*, 10. [CrossRef]
11. Han, Z.; Li, Q. Mendelian Inheritance of Orange Shell Color in the Pacific Oyster *Crassostrea gigas*. *Aquaculture* **2020**, *516*, 734616. [CrossRef]
12. Ge, J.; Li, Q.; Yu, H.; Kong, L. Mendelian Inheritance of Golden Shell Color in the Pacific Oyster *Crassostrea gigas*. *Aquaculture* **2015**, *441*, 21–24. [CrossRef]
13. Wan, S.; Li, Q.; Liu, T.; Yu, H.; Kong, L. Heritability Estimates for Shell Color-Related Traits in the Golden Shell Strain of Pacific Oyster (*Crassostrea gigas*) Using a Molecular Pedigree. *Aquaculture* **2017**, *476*, 65–71. [CrossRef]
14. Xu, C.; Li, Q.; Yu, H.; Liu, S.; Kong, L.; Chong, J. Inheritance of Shell Pigmentation in Pacific Oyster *Crassostrea gigas*. *Aquaculture* **2019**, *512*, 734249. [CrossRef]
15. Xu, L.; Li, Q.; Xu, C.; Yu, H.; Kong, L. Genetic Diversity and Effective Population Size in Successive Mass Selected Generations of Black Shell Strain Pacific Oyster (*Crassostrea gigas*) Based on Microsatellites and MtDNA Data. *Aquaculture* **2019**, *500*, 338–346. [CrossRef]
16. Xu, L.; Li, Q.; Yu, H.; Kong, L. Estimates of Heritability for Growth and Shell Color Traits and Their Genetic Correlations in the Black Shell Strain of Pacific Oyster *Crassostrea gigas*. *Mar. Biotechnol.* **2017**, *19*, 421–429. [CrossRef]
17. Ward, R.D.; English, L.J.; McGoldrick, D.J.; Maguire, G.B.; Nell, J.A.; Thompson, P.A. Genetic Improvement of the Pacific Oyster *Crassostrea gigas* (Thunberg) in Australia. *Aquac. Res.* **2000**, *31*, 35–44. [CrossRef]
18. Bentsen, H.B.; Olesen, I. Designing Aquaculture Mass Selection Programs to Avoid High Inbreeding Rates. *Aquaculture* **2002**, *204*, 349–359. [CrossRef]
19. Fjalestad, K.T. Selection methods. In *Selection and Breeding Programs in Aquaculture*; Gjedrem, T., Ed.; Springer: Dordrecht, The Netherlands, 2005; pp. 159–171. [CrossRef]
20. Williams, S.T. Molluscan Shell Colour. *Biol. Rev.* **2017**, *92*, 1039–1058. [CrossRef]
21. Mendoza, F.; Dejmek, P.; Aguilera, J.M. Calibrated Color Measurements of Agricultural Foods Using Image Analysis. *Postharvest Biol. Technol.* **2006**, *41*, 285–295. [CrossRef]
22. Yam, K.L.; Papadakis, S.E. A Simple Digital Imaging Method for Measuring and Analyzing Color of Food Surfaces. *J. Food Eng.* **2004**, *61*, 137–142. [CrossRef]
23. Li, L.; Xu, C.; Li, Q. Estimates of Genetic Parameters for Shell Color and Growth Traits in the Purple Shell Strain of Pacific Oyster (*Crassostrea gigas*) Based on Microsatellite Markers. *Aquaculture* **2025**, *599*, 742129. [CrossRef]

24. Stefenon, V.M.; Clauman, A.D. Genetic Divergence. *An. Acad. Bras. Cienc.* **2024**, *96*, e20230474. [CrossRef]
25. Iitembu, J.A.; Fitzgerald, D.; Altintzoglou, T.; Boudry, P.; Britz, P.; Byron, C.J.; Delago, D.; Girard, S.; Hannon, C.; Kafensztok, M.; et al. Comparative Description and Analysis of Oyster Aquaculture in Selected Atlantic Regions: Production, Market Dynamics, and Consumption Patterns. *Fishes* **2023**, *8*, 584. [CrossRef]
26. Helm, M.M.; Millican, P.F. Experiments in the Hatchery Rearing of Pacific Oyster Larvae (*Crassostrea gigas* Thunberg). *Aquaculture* **1977**, *11*, 1–12. [CrossRef]
27. Helm, M.M.; Bourne, N.; Lovatelli, A. *Hatchery Culture of Bivalves. A Practical Manual*, 471st ed.; FAO Fisheries Technical Paper: Rome, Italy, 2004; p. 177.
28. Ramos, C.D.O.; da Silva, F.C.; Gomes, C.H.A.d.M.; Langdon, C.; Takano, P.; Gray, M.W.; de Melo, C.M.R. Effect of Larval Density on Growth and Survival of the Pacific Oyster *Crassostrea Gigas* in a Recirculation Aquaculture System. *Aquaculture* **2021**, *540*, 736667. [CrossRef]
29. Moreira, H.G.; Sühnel, S.; Gomes, C.H.A.D.M.; Silva, E.; da Silva, F.C.; de Melo, C.M.R. Effect of Diet on Larval Settlement, Growth, and Spat Survival of the Oyster *Crassostrea gigas* (Thunberg, 1793). *Lat. Am. J. Aquat. Res.* **2024**, *52*, 521–535. [CrossRef]
30. Lima, R.D.C.D.; Ferreira, J.P.R.; do Espírito Santo, C.M.; da Silva, F.C.; Gomes, C.H.A.d.M.; Ramos, C.d.O.; Melo, C.M.R. de Spat of Pacific Oysters (*Crassostrea gigas*) Grown in Subtropical Environments. *J. Appl. Aquac.* **2024**, *36*, 342–364. [CrossRef]
31. Sühnel, S.; Picanço, T.; Medeiros, S.C.; Magalhães, A.R.M.; Demelo, C.M.R. Effects of Seeding Date and Seed Size on *Crassostrea gigas* (Thunberg, 1793) Culture in a Subtropical Climate. *J. Shellfish Res.* **2017**, *36*, 303–313. [CrossRef]
32. Zhang, Y.; Chen, Y.; Xu, C.; Li, Q. Comparative Analysis of Genetic Diversity and Structure among Four Shell Color Strains of the Pacific Oyster *Crassostrea gigas* Based on the Mitochondrial COI Gene and Microsatellites. *Aquaculture* **2023**, *563*, 738990. [CrossRef]
33. Li, M.; Tang, J.; Yuan, M.; Huang, B.; Liu, Y.; Wei, L.; Han, Y.; Zhang, X.; Wang, X.; Yu, G.; et al. Outer Fold Is Sole Effective Tissue among Three Mantle Folds with Regard to Oyster Shell Colour. *Int. J. Biol. Macromol.* **2023**, *241*, 124655. [CrossRef]
34. Chakraborty, S.K.; Singh, D.S.; Kumbhar, B.K. Influence of Extrusion Conditions on the Colour of Millet-Legume Extrudates Using Digital Imagery. *Ir. J. Agric. Food Res.* **2014**, *53*, 65–74. https://www.jstor.org/stable/24369736.
35. Hammer, Ø.; Harper, D.A.T.; Ryan, P.D. PAST: Paleontological Statistics Software Package for Education and Data Analysis. *Palaeontol. Electron.* **2001**, *4*, 4.
36. Instituto Brasileiro do Meio Ambiente e dos Recursos Naturais Renováveis. Portaria Nº 27, de 22 de Maio de 2003 [Ordinance IBAMA No 27, of May 22, 2003]. Diário Oficial Da União, Nº 98, Seção 1; Brasil, 2003. Available online: https://pesquisa.in.gov.br/imprensa/jsp/visualiza/index.jsp?data=23/05/2003&jornal=1&pagina=44&totalArquivos=80 (accessed on 22 September 2026).
37. Melo, C.M.R.D.; Silva, F.C.; Gomes, C.H.A.M.; Solé-Cava, A.M.; Lazoski, C. *Crassostrea gigas* in Natural Oyster Banks in Southern Brazil. *Biol. Invasions* **2010**, *12*, 441–449. [CrossRef]
38. Muniz, E.C.; Jacob, S.A.; Helm, M.M. Condition Index, Meat Yield and Biochemical Composition of *Crassostrea brasiliana* and *Crassostrea gigas* Grown in Cabo Frio, Brazil. *Aquaculture* **1986**, *59*, 235–250. [CrossRef]
39. Scaranto, B.M.S.; Ribolli, J.; Gomes, C.H.A.D.M.; Ferreira, J.P.R.; Melo, C.M.R. de Genetic Diversity of Parental and Offspring *Crassostrea gigas* through Gamete Pool Reproduction in Hatchery. *Acta Sci. Anim.* **2026**, *48*, e74706. [CrossRef]
40. Nell, J.A. The History of Oyster Farming in Australia. *Mar. Fish. Rev.* **2001**, *63*, 14–25.
41. Gjedrem, T.; Baranski, M. *Selective Breeding in Aquaculture: An Introduction*; Springer: Dordrecht, The Netherlands, 2009. [CrossRef]
42. Jiang, K.; Chen, C.; Jiang, G.; Chi, Y.; Xu, C.; Kong, L.; Yu, H.; Liu, S.; Li, Q. Genetic Improvement of Oysters: Current Status, Challenges, and Prospects. *Rev. Aquac.* **2024**, *16*, 796–817. [CrossRef]

Disclaimer/Publisher's Note: The statements, opinions and data contained in all publications are solely those of the individual author(s) and contributor(s) and not of MDPI and/or the editor(s). MDPI and/or the editor(s) disclaim responsibility for any injury to people or property resulting from any ideas, methods, instructions or products referred to in the content.